Carcinogenesis vol.31 no.9 pp.1661–1668, 2010
doi:10.1093/carcin/bgq106
Advance Access publication May 31, 2010

Hydroxyurea-induced global transcriptional suppression in mouse ES cells

Peng Cui[1,†], Qiang Lin[1,2,†], Chengqi Xin[1,2,†], Lu Han[3], Lili An[3], Yulan Wang[3], Zhishang Hu[3], Feng Ding[1], Lingfang Zhang[1,2], Songnian Hu[1,*], Haiying Hang[3,4,*] and Jun Yu[1,*]

[1]CAS Key Laboratory of Genome Sciences and Information, Beijing Institute of Genomics, Chinese Academy of Sciences, No.7 Beitucheng West Road, Chaoyang, 100029 Beijing, China, [2]Graduate School of Chinese Academy of Sciences, 100029 Beijing, China, [3]Center for Computational and Systems Biology and [4]National Laboratory of Biomacromolecules, Institute of Biophysics, Chinese Academy of Sciences, 15 Datun Road, Chaoyang District, Beijing 100101, China

*To whom correspondence should be addressed. Tel: +86 10 82995362;
Fax: +86 10 82995362;
Email: husn@big.ac.cn
Correspondence may also be addressed to Haiying Hang.
Tel: +86 010 6488-8473;
Email: hh91@sun5.ibp.ac.cn

Hydroxyurea (HU), as a therapeutic medicine, has been extensively used clinically. To further survey molecular mechanisms of HU treatment, we analyzed global transcriptomic alteration of mouse ES cells in response to the treatment using high-throughput sequencing. We show that the global transcriptional activity is significantly suppressed as cells are exposed to HU treatment and alters multiple key cellular pathways, including cell cycle, apoptosis and DNAs. HU treatment also alters alternative splicing mechanisms and suppresses non-coding RNA expression. Our result provides novel clues for the understanding of how cells respond to HU and further suggests that high-throughput sequencing technology provides a powerful tool to study mechanisms of clinical drugs at the cellular level.

Introduction

Hydroxyurea (HU) as a clinical therapeutic medicine has been extensively used for treating hematological malignancies, chronic myelogenous leukemia, sickle-cell anemia, carcinomas and other diseases (1–3). One mechanism of its action is to effectively increase fetal hemoglobin expression for sickle-cell disease treatment through a HU-derived NO pathway (4). Another is believed to reduce production of deoxyribonucleotides via inhibition of ribonucleotide reductase by scavenging tyrosyl free radicals; such an action is capable of arresting DNA replication and preventing cell cycle progression through S phase (5). HU has also been reported to be genotoxic and induces DNA damage and is thus believed to be a carcinogen (6,7).

To further survey the effect of HU treatment to the cell and to understand its molecular mechanism, we used the recently developed RNA-seq method (8) and mouse embryonic stem cells (ESCs) to interrogate the dynamics of the transcriptomes when subjected to HU treatment. Our data demonstrated a reduced transcriptional activity in the whole genome scale, including coding and non-coding regions, leading directly to the downregulation of thousands of genes involved in important functional pathways. The disturbance of multiple functional pathways other than the known effects on cell cycle includes apoptosis and DNA repair. The new data also allow us to postulate molecular mechanisms of HU treatment and to show the power of new sequencing technology.

Abbreviations: AS, alternative splicing; cDNA, complementary DNA; ESC, embryonic stem cell; HU, hydroxyurea; PI, propidium iodide; PCR, polymerase chain reaction; TGF, transforming growth factor.

[†]These authors contributed equally to this work.

Materials and methods

Cell culture and flow cytometry analysis

S129 mouse nES cells and hnES cells were grown in medium according to the previous method (9). hnES cell was cultured in the presence of hydroxycarbamide at a concentration of 1 mM.

Cell cycle and apoptosis assays

The expression profile of cells in different phases of the cell cycle was determined using previously established methods (10). Cells were collected, stained with propidium iodide (PI) and analyzed with a FACSCalibur (Becton Dickinson). For apoptosis analysis, cultured cells were trypsinized for 10 min using 0.1% trypsin at 37°C (Sigma), washed twice with cold phosphate-buffered saline and resuspended in 1× binding buffer [10 mmol/l *N*-2-hydroxyethylpiperazine-*N′*-2-ethanesulfonic acid (pH 7.4), 140 mmol/l NaCl and 2.5 mmol/l $CaCl_2$] at a concentration of 1×10^6 cells/ml. Cells were stained with Annexin V-FITC (Jingmei Biotech) and PI for 15 min at room temperature before flow cytometric analysis.

Assessment of DNA damage by histone 2AX phosphorylation

Cells (1×10^6) were fixed in ice-cold 70% ethanol, incubated with 1% bovine serum albumin, 0.25% Triton X-100 in Tris-buffered saline for 15 min on ice and stained with primary anti-γ-H2AX antibody (Bethyl) at 1:500 overnight at 4°C. The cells were stained with a secondary goat anti-mouse Ig (H+L)-FITC (Jackson ImmunoResearch Laboratories, West Grove, PA) at 1:400 for 30 min at room temperature and counterstained with 5 μg/ml PI containing RNAse A for 30 min and analyzed with flow cytometry.

Comet assays

The protocols published by Singh *et al.* (11) and Olive *et al.* (12) were used with minor modifications. The alkaline comet assay monitors both DNA single- and double-strand breaks, whereas the neutral comet assay detects only double-strand breaks. As for the alkaline comet assay, the slides were precoated with a thin layer of 1% normal melting agarose and allowed to dry. Single cell suspensions of either HU-treated or control cells were harvested and resuspended to 500 000 cells/ml. Twenty microliters of each final suspension was added to 80 μl of premelted 0.75% low-melting-point agarose and was spread onto a precoated slide. After solidification, the slides were placed in alkaline lysis solution and the cells were lysed in the dark at 4°C for 2 h. Slides were then placed in alkaline buffer in the dark at 4°C for 20 min to allow for unwinding of the DNA. The slides were subjected to electrophoresis at ∼0.74 V/cm for 20 min. Following electrophoresis, the slides were rinsed with neutralization buffer and then stained with PI. Fluorescence images for at least 50 nuclei were captured using a microscope and analyzed by CASP-1.2.2 software (University of Wroclaw) for tail moment (the geometric mean of fluorescence on the tail from the nucleus). The neutral comet assay is identical to the alkaline comet assay except that after solidification, the slides were placed in neutral lysis solution and the cells were lysed in the dark at 4°C for 2 h. Slides were placed in 1× TBE buffer in the dark at 4°C for 30 min to allow unwinding of the DNA and subjected to electrophoresis in 1× TBE buffer at 1.0 V/cm for 20 min subsequently.

Western blotting and qRT–polymerase chain reaction assay

Western blotting was performed based on a previously published protocol (13) except a specific antibody, anti-Oct4 antibody (AF1759; R&D Systems, Minneapolis, MN) was used to probe mouse ES cells. For qPCR analysis, total RNA was extracted based on the Trizol protocol (cat.10837-08; Invitrogen), treated with DNAase I and reverse-transcribed to complementary DNA (cDNA) (random priming) by using a standard protocol (SuperScript II reverse-transcriptase; Invitrogen). cDNA was diluted to 150 ng/μl and qRT–polymerase chain reaction (PCR) reaction volume is 20 μl (SYBR Green, TFP202; TIANGEN).The condition for qRT–PCR is as follows: the initial denaturation at 95°C for 1.5 min and 40 amplification cycles at 95°C for 15 s, 60°C for 15 s and 68°C for 40 s.

RNA-seq library and sequencing

We used Trizol to isolate total RNA from the cultured cells and deplete rRNA by using the Ribo-minus Eukaryote kit from Invitrogen (cat.10837-08), based on in part the protocol from SOLiD™ Small RNA Expression Kit (#4397682) with a starting material of 1 μg rRNA-depleted RNA. Briefly, we put together the following mixture on ice in order: 8 μl RNA (1 μg), 1 μl 10× RNase III buffer and 1 μl RNase III (#AM2290; Applied Biosystems). The mixture was

incubated at 37°C for 10 min followed by another incubation period at 65°C for 20 min. We use FlashPAGE™ to collect fragmented RNA in a length range of 50–150 bp and to purify the RNA by using FlashPAGE Reaction Clean-Up Kit (#AM12200; Applied Biosystems). We resuspend the air-dried RNA in 3 µl nuclease-free water and the ligation mixture was put together, which contains the RNA, Adaptor Mix and Hybridization Solution. The ligation was started by adding ligase to each sample and the mixture was incubated at 16°C for 16 h. cDNA was synthesized by adding 20 µl RT master mix to each sample and incubated at 42°C for 30 min. The RNA residues were removed with RNase H (10 U in 10 µl cDNA mixture) at 37°C for 30 min. The cDNA library was amplified, cleaned with Qiagen MinElute PCR purification Kit (#28004, 28006; Qiagen) and purified on a native 6% polyacrylamide gel. Usually 400 µl reaction product is enough for sequencing and a fraction of the library in a size range of 140–200 bp (DNA ladder, #10821-015; Invitrogen) is usually selected for SOLiD sequencing.

Sequence read mapping

We used the mouse reference sequence (release mm9, July 2007) from UCSC for read mapping, which contains 21 896 genes. We also constructed an Exon–exon Junction Database for gene mapping with 34 nt flanking sequences into both the donor and acceptor sequences. Low-quality reads (with the average quality value <8) were filtered and the remaining reads were used for further mapping steps. We mapped the full length 35 bp reads to the reference, analyzed the flow-through against our junction database and repeated the first and the second steps for the first 30 and 25 bp truncated reads (after removal of the tag sequences beyond 30 bp and 25 bp). rRNA read filtering was performed at the beginning of read mapping with different length. For the junction and 25 bp mapping, we allowed two and three mismatches for 30 bp and 35 bp, respectively.

Gene expression analysis

We measured gene expression by read count that is normalized with the total mapped reads and gene length with 'Rpkm' method (14). GenMAPP 2.0 was used for showing differential expressions in different pathways (15). For each class of repeat elements annotated based on RepeatMarker, we counted the total reads mapped to the repeat regions and normalized the data with the total mapped reads from two libraries. We isolated RNA from nESC and hnESCs and hybridized with Mouse Genome 430 2.0 Array and analyzed using DNA-Chip Analyzer (16). The fifth percentile (PM-only) was used as the background and the average value was used for Refseq genes with different probes.

Transcripts from non-coding regions

We collected the mouse ncRNA annotation data from the publically available ncRNA databases that include ncRNAdb, RNAdb, fRNAdb, FANTOM3, NONCODE, Refseq and Ensembl. Transcripts in the length of <50 bp were excluded from our analysis. We use blat to map sequences, using a criterion of match-length/inquiry-length $\geq$ 0.9 and mismatch-length/inquiry-length $<$ 0.1. Transcripts mapped to >20 loci were considered to be repeats and discarded. We annotated 3943 ncRNA loci (for ncRNA, RMAdb, fRMAdb and NONCODE databases). After combined with FANTOM3, Refseq and Ensembl data, we eliminated redundant annotation and all loci were named according to our database rank (Ensembl>Refseq>fRNAdb>NONCODE->NCBI->ncRNAdb->FANTOM3) and divided into following group: miRNA, miscRNA, snRNA, snoRNA, rRNA, tRNA, mRNAlike, FANTOM, retrotransposed, scRNA and others belong to 'database-other'. We compared the reads mapped sites and ncRNA coordinates to estimate ncRNA expression affected by HU treatment.

Identification of novel non-coding transcripts

All mapped reads without shared sequences with known ncRNAs and gene regions are collected. We clustered the reads for overlaps and mapped them further by allowing gaps (maximum gap > 500 bp). We also set criteria to exclude possible artifacts as follows: (i) for short regions (length <200 bp and >50 bp in length), we asked for at least five reads, (ii) for long segments, we limited the intensity to be $\geq$0.02 or with greater than five reads. We looked into novel transcription regions that have 50% sequence overlap between the two libraries. For Refseq defined genes, we used IDEG6 to define differentially expressed genes ($P < 0.01$).

Results

Suppressed global transcription in HU-treated ESCs

To systematically assess the transcriptomic alternations in a genome-wide fashion when cellular DNA is exposed to 1 mM HU for 12 h, we used the ribo-minus RNA-sequencing (rmRNA-seq) method to acquire transcriptional profiles from both HU-treated and untreated ESCs (nESCs and htESCs) at single-nucleotide resolution (see the experimental procedures for details). Based on our previous study using the same cells (17), we found that HU treatment in a dosage of 1 mM for 12 h was able to block almost all the cells in S phase and did not cause cell death in significant numbers. This dosage also induced maximal S/M checkpoint activation if the checkpoint genes were intact from the same study. Therefore, we used this HU dosage in this study to induce strong biological effects and also to avoid cell death that would complicate our analysis on the HU-induced changes in gene expression. We took the number of reads as a general surrogate for transcriptional activity. From the rmRNA libraries of nESC and htESC, we generated ~26 million mapped reads (~35 bp in length), using the ABI SOLiD sequencing system (Table I). From the nESC library, we generated 63% (8 081 450) uniquely mapped reads to genomic loci, where these mapped reads were almost evenly distributed among exons (32%), introns (32%) and intergenic sequences (34%). In sharp contrast, 48% (6 233 604) uniquely mapped reads from the htESC library, their genomic distributions were 26, 20 and 52% among exonic, intronic and intergenic regions, respectively (Table I).

The total uniquely mapped reads in htESC library are also reduced nearly 28% when compared with those in the nESC library, and such a reduction of transcriptional activity occurs across almost all regions of the genome: exonic (Figure 1A), intronic (Figure 1B) and intergenic (Figure 1C and D) albeit more prominent in exonic and intronic regions. In the exonic regions, read counts were significantly reduced among chromosome 1, 3, 13, X and Y, and the degree of reduction varied from chromosome to chromosome, typically between 7 and 43% in nESCs (Figure 1A). In the intronic regions, the reduced read counts were seen in all chromosomes with the degree of reduction ranging from 15 to 77% in nESCs (Figure 1B). The change of transcription activity in the intergenic regions is striking; we observed that about half of the chromosomes (1, 4, 5, 6, 11, 12, 14, 16 and 17) in htESCs show elevated transcription activity, especially chromosomes

Table I. Tag mapping summary

Read mapping	nESCs	htESCs
Raw reads	124 844 521	74 145 307
High-quality reads	104 635 294	64 669 436
Reads after filtering rRNAs	95 902 214	46 121 313
Mapped reads	12 857 969	13 018 383
Reads mapped to unique loci (/mapped)	8 081 450 (62.85%)	6 233 604 (47.88%)
Reads mapped to multiple loci (2–10) (/mapped)	2 692 911 (20.94%)	4 524 110 (34.75%)
Reads mapped in high redundancy (>10) (/mapped)	2 083 608 (16.20%)	2 260 669 (17.37%)
Exon–exon junction reads	320 572	222 078
Unique reads mapped to exons	2 604 760 (32.23%)	1 610 343 (25.83%)
Unique reads mapped to introns	2 504 938 (32.00%)	1 265 648 (20.30%)
Unique reads mapped to intergenic regions	2 793 866 (34.57%)	3 253 114 (52.19%)
Unique reads mapped to exon–intron junctions	177 886 (2.20%)	104 499 (1.68%)

4, 6 and 17 (Figure 1C). Further inspection on absolute counts for the reads revealed that the increase was due to a higher number of upregulated reads of 15 non-coding RNAs from these chromosomes (supplementary Table S1 is available at *Carcinogenesis* Online). When these genomic regions were excluded from the dataset, the read counts unique to the intergenic regions were actually reduced in all 21 chromosomes of htESCs (Figure 1D). This is also evident from the inspection of the whole genome in a sliding window (Figure 2; supplementary File 1 is available at *Carcinogenesis* Online). Some large contiguous genomic segments were characterized as transcriptional repressing or silencing in htESCs but highly expressed in nESCs and such segments were observed in both genic and intergenic regions (Figure 2).

Gene expression profile

Inspecting regions that are active in both nESCs and htESCs, we often found lower transcription activities in htESCs. To test this possibility, we analyzed the expression level of all genes transcribed in nESCs and htESCs. We first calculated gene activity by counting the number of reads mapped to exons of each RefSeq-defined gene. Using the

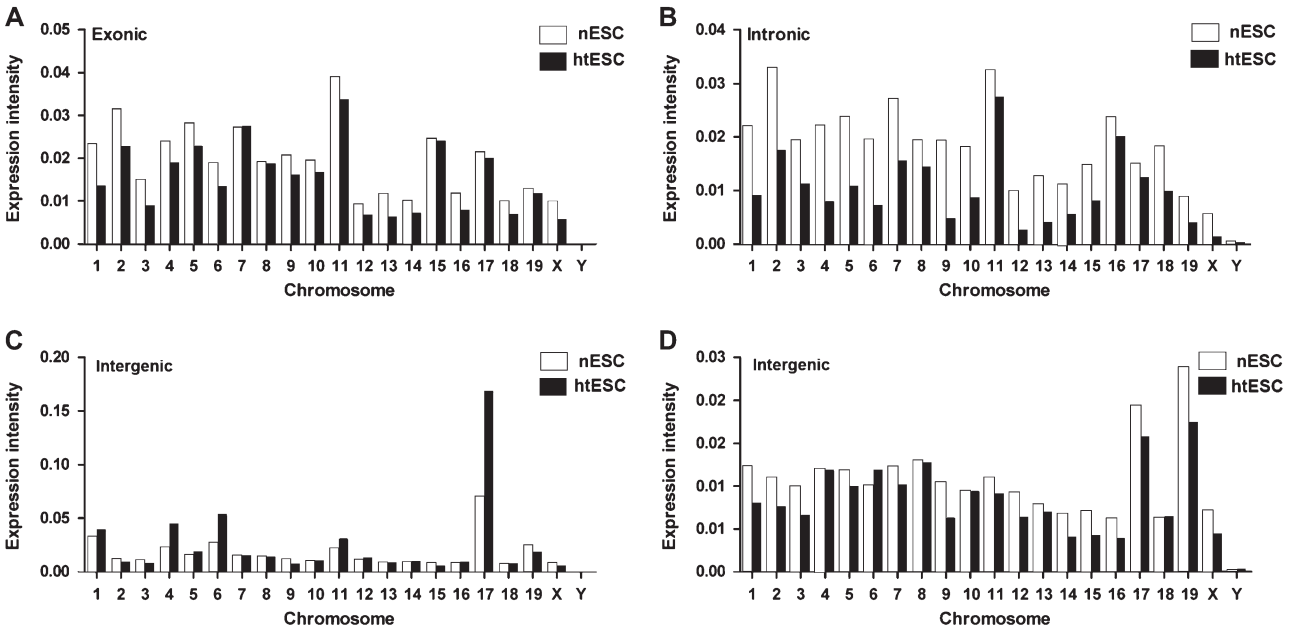

Fig. 1. Read counts (expression intensity) of mouse chromosomes. Comparison of the expression intensity of each chromosome between nESC (pink) and hnESC (blue) are summarized for (**A**) exon, (**B**) intron, (**C**) intergenic and (**D**) intergenic regions without the overexpressed parts. The expression intensity is determined by the ratio of mapped reads in each chromosome over total mapped reads. Transcription ability attenuates at intronic regions response to DNA damage. The obviously expression change in the intergenetic sequences of chromosome 17 is the result of unusual overexpression regions (39979937–39985743) including miRNAs, SSU_rRNAs and pseudogenes.

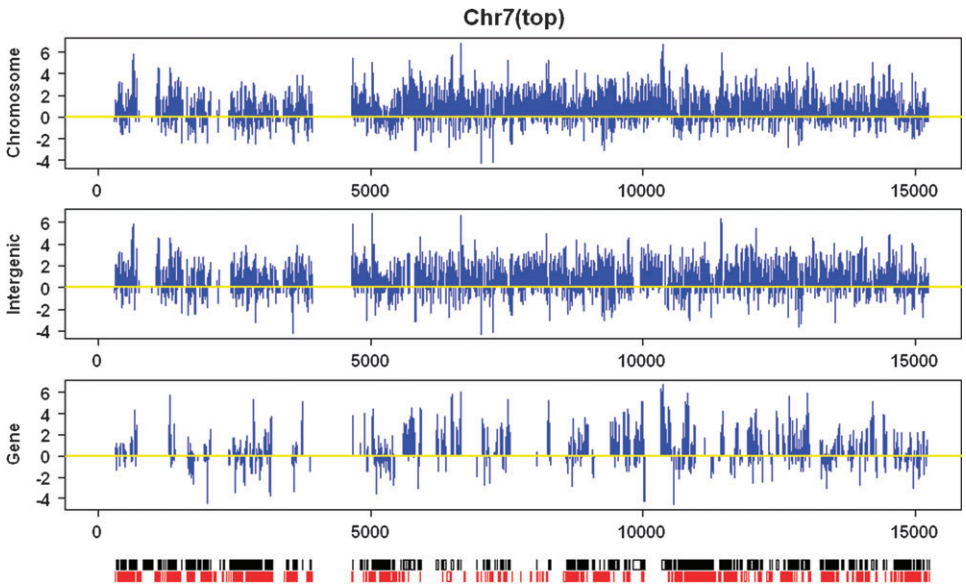

Fig. 2. Transcription loci on the top strand of chromosome 7. We used a 100-k window and 10-k sliding step for the analysis. In each sliding window, the relative expression value (vertical bars) is the ratio of mapped reads normalized over the total mapped reads in the nESC and hnESC libraries. We did a log2 transformation for the values and the upregulated expressions in nESCs are placed above the yellow bar and those from hnESCs are placed below. A bar graph indicating Ref-seq gene positions in two strands is shown at the bottom. Data from other chromosomes are summarized in supplementary File 1, available at Carcinogenesis Online.

threshold of five reads per gene, we identified 14 830 and 14 517 RefSeq-defined genes expressed in nESCs and htESCs, respectively. Furthermore, we analyzed the differentially expressed genes between nESCs and htESCs, evaluated the result based on a Poisson model and identified 6262 differentially expressed genes ($P < 0.01$ and 2-fold change) with 1126 upregulated and 5136 downregulated genes in nESCs and htESCs, respectively. This result indicates that most differentially expressed genes (82%) are downregulated in htESCs, consistent with the global transcriptional suppression as a result of HU treatment.

In order to confirm this conclusion, we validated our results based on a parallel study by using Affymetrix microarrays and qRT–PCR. The two platforms of RNA-seq and microarrays showed a strong correlation (Pearson coefficient $r_{nESC} = 0.73$ and $r_{hnESC} = 0.57$; $P < 0.0001$) in identifying expression profiles in the two samples (supplementary Figure S1AB is available at *Carcinogenesis* Online). We cross-mapped the differentially expressed genes identified based on both methods and found that microarray data supported our conclusions derived from RNA-seq data (supplementary Figure S1CD is available at *Carcinogenesis* Online). From the microarray data, we detected 12 464 and 13 078 RefSeq-defined genes expressed in nESCs and htESCs, respectively (supplementary Figure S2 is available at *Carcinogenesis* Online), so that the microarray data discovered significantly less number of genes as compared with the RNA-seq method (14 830 and 14 517 in nESCs and htESCs). The most undetected genes in microarrays are poorly expressed in the RNA-seq library (supplementary Figure S3 is available at *Carcinogenesis* Online), such as *wnt3a*, *itgb4*, *prph* and *cacna1g*, which are involved in Wnt, cell communication and calcium signal pathways, and significantly upregulated in htESCs. For qRT–PCR assay (detail result see supplementary file 2, available at *Carcinogenesis* Online), we randomly selected 77 genes for validation and 38 of them showed similar gene expression patterns as what were found by sequencing. Most genes that failed to be validated in qRT–PCR are poorly expressed. The correlation of relative genes expression between rmRNA-seq and qRT–PCR was 0.93.

The suppression of ncRNAs in htESCs

To assess the transcriptional status of non-protein-coding genes in response to the HU treatment, we analyzed the transcriptional activity of both known and novel ncRNAs (defined in methods) between nESCs and htESCs. First, using the threshold of five reads per locus, we identified 12 425 known ncRNAs transcribed in nESCs as compared with 5782 in htESCs. Among them, 5350 ncRNAs are common in both cell libraries, and 7075 and 432 ncRNAs are unique to nESCs and htESCs, respectively (supplementary Figure S4 is available at *Carcinogenesis* Online). This result suggests that there are more silenced ncRNAs in htESCs. In addition, analyzing differential expression of these common ncRNAs, we found that most ncRNAs are downregulated in htESCs (supplementary Figure S4 is available at *Carcinogenesis* Online). This result is consistent with the reduced read counts within intergenic regions. In summary, similar to the case of protein-coding genes, the non-coding regions also showed reduced transcriptional activities in htESCs as an effect of relatively poor transcriptions in both the active and inactive regions. Based on our criteria, we also identified 11 041 and 3745 novel ncRNA transcripts in nESCs and htESCs, respectively.

Despite the fact that a global transcriptional activity reduction of ncRNAs is observed in htESCs, which is considered as the result of transcriptional repression, we still identified 257 known ncRNA loci that are significantly upregulated in htESCs, and the transcriptional regulation of these ncRNAs are biased among chromosome locations. Of them, 24% (61) were identified as snoRNA, a class of small RNA molecules that guide chemical modifications (methylation or pseudouridylation) of ribosomal RNAs and other RNA genes (tRNAs and other small nuclear RNAs). The expression level variation of these snoRNAs suggested that certain RNA biosynthesis pathways may be disturbed by HU-treatment condition, consistent with previous findings that snoRNA activity can be upregulated under stress conditions (18). In addition, we identified some retrotransposons and ncRNAs (176) showing an elevated transcriptional activity. Recent studies suggested that retrotransposons and ncRNAs could contribute to transcriptional regulation of their neighboring genes via epigenetic mechanisms in eukaryotes, such as transcriptional interference and antisense silencing (19). To test this possibility in htESCs, we correlated the expression of upregulated retrotransposons and ncRNAs with that of the nearest upstream or downstream genes and found 64% (113) of the upregulated retrotransposons and ncRNAs correlated with the expression changes of their nearby genes. Several illustrative examples are shown in supplementary Figure S5 (available at *Carcinogenesis* Online).

Elevated expression of snRNA and srpRNA in htESCs

To better describe the transcriptional status in response to HU stress, we further surveyed the change of repeat expression. In nESCs, we found ~26% (3 327 998) of all mapped reads in nESCs are within the repeat elements defined with Repeatmasker, as opposed to 44% (5 720 215) of those in htESCs; the expression of repeat sequences increased by 70% in htESCs when compared with that of nESCs. Furthermore, when separating repeat sequences into different classes, such as satellite repeat, LINE, SINE, LTR, snRNA and srpRNA (supplementary Figure S6 is available at *Carcinogenesis* Online), we found that the transcriptional activity of satellite repeat, LINE, SINE and LTR are reduced in htESCs but snRNA and srpRNA showed significantly higher transcriptional activity in htESCs, which was identified as the major contributors to the elevated expression of repeat sequences. snRNAs, a class of small RNA molecules functioning in the nucleus of eukaryotic cells, are mainly involved in RNA splicing by forming small nuclear ribonucleoproteins (20). srpRNA is the RNA component of signal recognition particle, required for co-translational protein targeting to endoplasmic reticulum membranes. This significant upregulation of the two special classes of RNA in htESCs suggests possible involvement of both transcriptional and translational level regulation in response to HU stress.

The effect of DNA damage on alternative splicing

Since DNA damage may affect alternative splicing (AS) through inhibiting RNA polymerase II elongation (21), we investigated the changes of AS genes between nESC and htESC after HU treatment. We observed 2237 AS events in 1260 genes and 1549 AS events in 935 genes expressed in nESC and htESC (with criterion of more than two reads per AS), respectively. Among them, 563 AS events of 362 genes are common in both samples and 2660 AS events of 1565 genes are associated with HU treatment. Analyzing differentially expressed genes, we found that 62% (8713 genes, $P < 0.01$) genes change their expression levels upon HU treatment; of which 77% (6734 genes) appeared downregulated and 23% (1979 genes) showed upregulations. Moreover, the proportion of genes that display AS events is substantially higher among the genes experiencing changes in expression (1303/8713, 15%) than among the genes that are not affected at the expression level (381/5317, 7%). The genes showing AS changes upon HU treatment are listed in supplementary Table S2 (available at *Carcinogenesis* Online). Our result is consistent with the key feature of DNA-damage responses—coupling to AS through transcription suppression.

Functional implications

Previous studies indicated that HU alters cell cycle and apoptosis as well as causes DNA damage (6,22,23). To correlate our data to these cellular processes, we further analyzed functional categories and pathways of the expression-suppressed and upregulated genes in htESCs, coupled with flow cytometry analyses.

Cell cycle. HU, as a well-studied activator of the S-phase checkpoint, stalls replication forks by depleting the deoxynucleotide triphosphate pool, leading to the arrest of cell cycle at G_1/S border and within S phase (5). Therefore, we first analyzed the change of transcriptional

activities for genes involved in cell cycle regulation after HU treatment (Figure 3). At the G_1 phase, we observed that *cdkn1a* (*p21*) and *cdkn2a* (*p16*)/*cdkn2b* (*p15*), the major regulators of cell cycle progression, showed significant upregulation in htESCs, and their elevated expression level inhibits the activity of cyclin-dependent kinases and thus arrested cell cycle at G_1/S border and within S phase (24–26). This upregulation of *p21* is consistent with previous reports that the transcription of *p21* could be activated by a variety of stress stimuli (22). Since the current view pointed to the transforming growth factor (TGF)-β signaling pathway for *p15* control (27), we looked at the genes encoding THBS1/THBS4, TGF-β, TGFR-2 and SMAD3 and found that they are all upregulated significantly in htESCs (28–30) (supplementary Figure S7 is available at *Carcinogenesis* Online).

In addition, the genes encoding cyclin-dependent kinases, such as *cdk2*, *cdk4* and *cdk6* (31), showed significant downregulation in htESCs, marking the blockage of the cell cycle progress. Further analysis discovered that some genes as necessaries of S phase, such as the genes encoding ORC (origin recognition complex), MCM (mini-chromosome maintenance) and E2F (transcriptional factor for activating the S-phase-related gene transcription) are all downregulated in htESCs, which are major regulatory factors contributing to the stalling at G_1/S border and within S phase. Furthermore, other genes from G_2 and M phase, such as *ccna2* (32) and *ccnb2*, are downregulated in htESCs, consistent with our flow cytometry data that the number of cells are reduced in G_2 and M phase (11%), whereas the number of cells in G_1 phase is increased dramatically (∼19%) after HU-treatment for 12 h (Figure 4).

Apoptosis. Although it has been shown that HU treatment induces apoptosis (22), precise mechanisms of its action is yet to be demonstrated. Based on the apoptosis regulation network, we observed that genes including *tradd*, *traf2*, *nfkb1*, *jun* and *trp73* are upregulated in htESCs (supplementary Figure S8 is available at *Carcinogenesis* Online), which are involved in the tumor necrosis factor pathway for initiating cell apoptosis; their upregulation initiates and promotes apoptosis in htESCs (33,34). This result suggested a possible mechanism for HU-mediated cell death involving the TNF–TRADD–TRAF2 pathway (35). In this pathway, we found that *nfkbia* is upregulated, which bind to the nuclear factor-kappaB complex

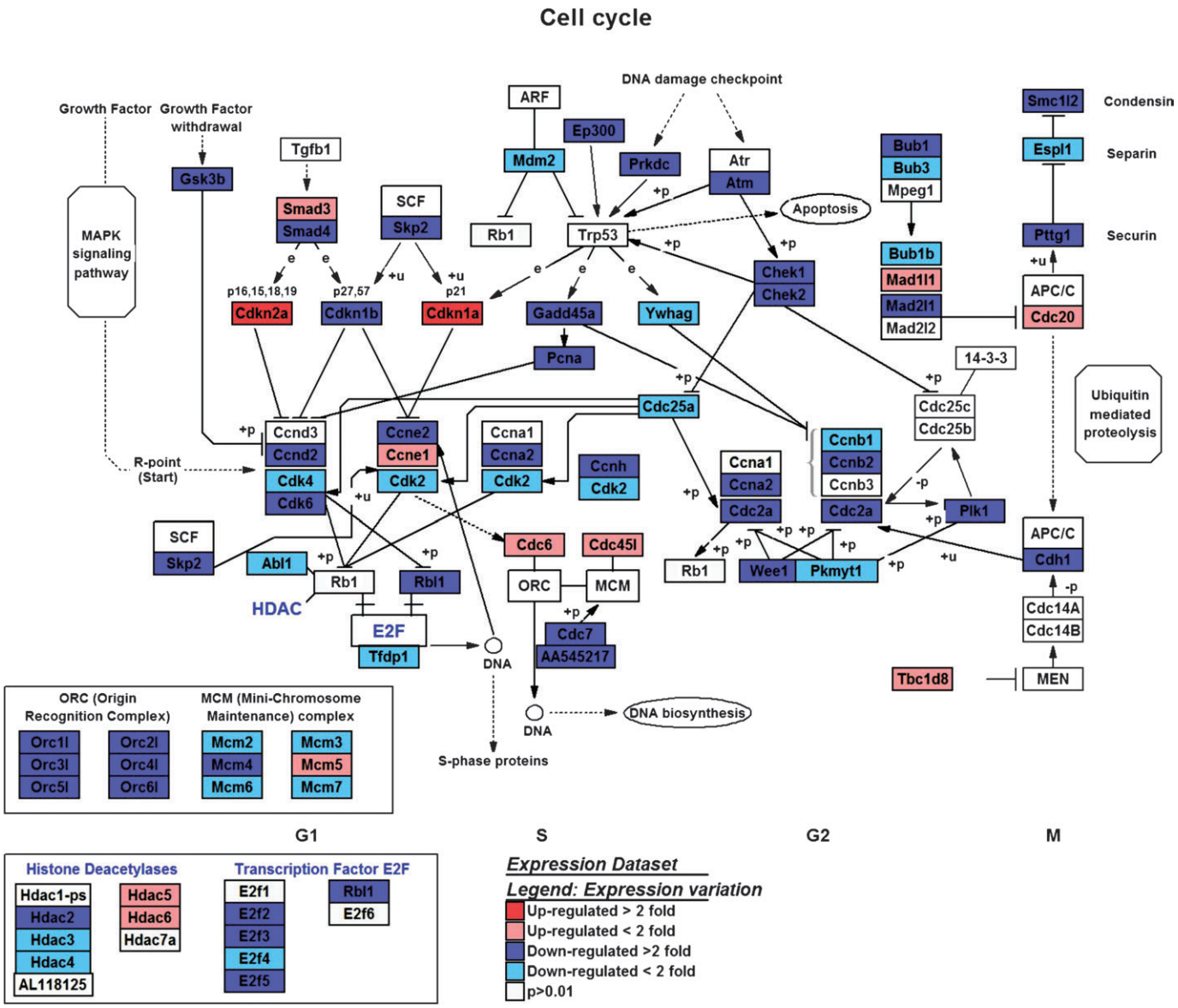

Fig. 3. Relative gene expressions in GenMAPP cell cycle pathways referenced to RNA-seq data. Differentially expressed genes are colored according to fold changes. We used the criterion of $P < 0.01$ to index the genes.

resisting apoptosis-induced processes (36,37). Moreover, the genes *bax*, *bbc3* and *bok*, encoding the proteins for mitochondrial outer membrane permeabilization, were also found upregulated in htESCs, which may promote the release of cytochrome c and activate the cell apoptosis pathway (38,39). These findings indicated that factors involved in both promoting and resisting cell apoptosis may influence htESCs. We also used flow cytometry to analyze the effect of HU treatment on cell apoptosis and observed that the number of cells undergoing apoptosis increased ~4% after HU treatment (Figure 5).

DNA damage repair. As a clinical drug, HU exerts cytotoxic pressure on cells and induces DNA damages via base oxidation. We reanalyzed DNA damage in HU-treated cells using flow cytometry (supplementary Figure S9 is available at *Carcinogenesis* Online). We found that the number of H2AX-γ-positive cells increased significantly in the population of htESCs, indicating increased DNA double-strand breaks. We also monitored DNA double- and single-strand breaks with neutral (double-strand breaks) and alkaline (both single- and double-strand breaks) comet assays, and both assays showed significant increase of DNA lesions (Figure 6). The number of total breaks detected by alkaline comet assay is much more than that of double-strand breaks monitored by neutral comet assay (Figure 6C), thus HU treatment led to much more single-strand breaks than double-strand breaks. Based on our RNA-seq data, we found that many DNA damage repair enzymes are upregulated in htESCs, including *trex1*, *mus81*, *nthl1* and *xrcc1* (supplementary Figure S10 is available at *Carcinogenesis* Online). *Trex1*, *mus81* and *nthl1* all encode endonucleases that may be used for repairing HU-induced stalls in the replication fork and oxidized pyrimidine residues (40–42), whereas *xrcc1* encodes a protein involved in efficient repair of DNA single-strand breaks (43,44). *Trex1* is also a 3′ to 5′ exonuclease to degrade DNA when cells are dying (42). Their upregulation suggests the pathways of DNA damage repair are activated when ESCs are exposed to the genotoxic stress (such as HU) and further confirms that HU, as potential carcinogen, can lead to stalls in the replication fork, base oxidation and DNA single- or double-strand breaks.

Other biological processes related to HU treatment. In addition to the known effects of HU treatment on cell cycle, apoptosis and DNA damage, we also discovered that a few other important biological processes including RNA synthesis and processing, cell communication-related pathways, Hedgehog-induced Wnt, Hedgehog signaling

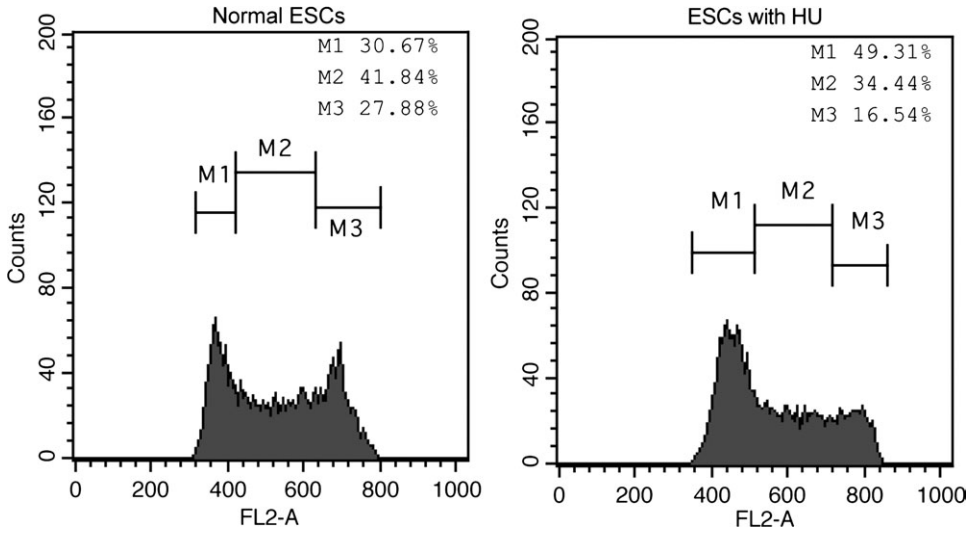

Fig. 4. HU induces G_1-phase checkpoint. Cultured with HU (2 mM) for 12 h, G_2/M phase cells (before HU treatment) move out of G_2/M phase and most cells are blocked at the G_1 phase.

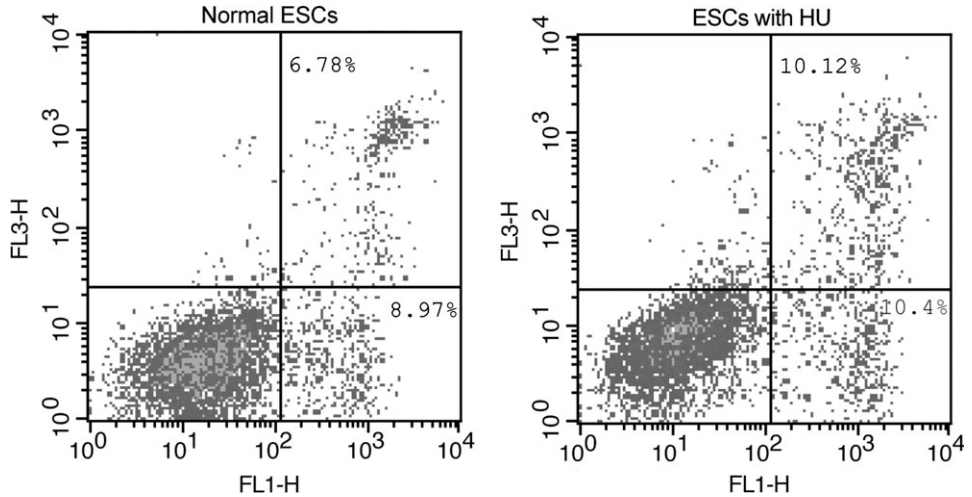

Fig. 5. Annexin V expression for HU-treatment induced apoptosis analysis. FL1H (horizontal) and FL3H (vertical) show the intensity of Annexin V-FITC and PI straining, respectively. The lower and upper right quadrants represent early apoptotic cells and induction of later apoptotic or necrotic cells, respectively. Populations of apoptotic cells (%) are labeled in both quadrants. After HU treatment, a significant fraction of the cells underwent apoptosis.

pathways and calcium signaling pathway can be significantly disturbed by HU treatment. In RNA synthesis and processing, several transcriptional factors, such as TAFs, GTFs and *ccnh* (45–48), related to messenger RNA maturation were found downregulated in htESCs (supplementary Figure S11 is available at *Carcinogenesis* Online), suggesting direct effects of HU-treatment on transcription. We further found that most genes involved in ECM-receptor interaction (49,50) are significantly upregulated after HU treatment (supplementary Figure S12 is available at *Carcinogenesis* Online). Last but not least, in the Hedgehog-induced Wnt, Hedgehog and calcium signaling pathways (supplementary Figure S13 is available at *Carcinogenesis* Online), we observed that many genes are significantly upregulated in htESCs, which suggests that these signaling pathways may also be activated. Wnt and Hedgehog signaling pathways are believed to play many roles in cell proliferation, cell cycle, cell apoptosis, embryogenesis and cancer (51,52); their activation suggests the important effects of HU treatment on cellular proliferation and tumorigenesis. Calcium signaling pathway is used for regulating the import of from outside the cell; its change indicates that HU may alter the import of calcium through direct or indirect actions. It is noteworthy that as much as 40% upregulated genes are concentrated among these pathways, suggesting that HU treatment may specifically affect these processes. Other independent experimental data are needed to validate these discoveries in the future.

As mouse ES cells were used for this study, an obvious question raised is whether these differentially expressed genes stemmed from the differentiation caused by the defined HU treatment condition: 1 mM for 12 h. To answer this question, we analyzed Oct4 levels in the mouse ES cells before and after HU treatment by western blotting and did not find any decrease of Oct4 expression (Figure 7). The result suggested that HU did not induce cell differentiation under this experimental condition.

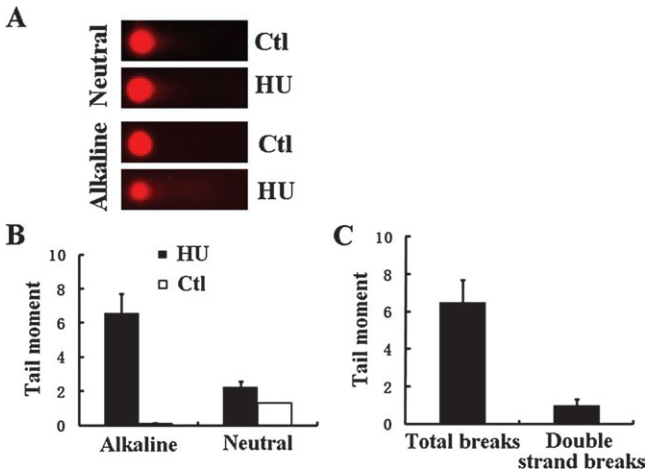

Fig. 6. HU treatment induces single- and double-strand breaks in DNA. We show typical examples of comets (**A**) and a comet measured as tail fluorescence geometric mean that quantifies the extent of DNA damage (**B**) and the tail moment (**C**) that equals to tail moment of HU-treated cells (HU) minus tail moment of control cells (Ctl).

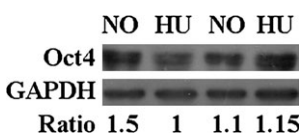

Fig. 7. HU treatment does not induce mouse ESC differentiation. Two independent sets of mock-treated and HU-treated (1 mM HU for 12 h) ESCs were used for western blotting analysis to detect Oct4 (a typical mark for undifferentiated cells) expression and we did not observe reduction of Oct4 expression.

Discussion

In this study, we interrogated gene expression of mouse ESCs upon HU treatment based on high-throughput sequencing data and discovered several key characteristics. First, we noticed reduced global transcriptional activity in both genic and intergenic regions in htESCs, which is associated with the typical transcription response to DNA damage—ubiquitylation- and proteasome-mediated degradation of RNA polymerase II generally occur under the condition of DNA damage, leading to transcription inhibition (53). However, to our surprises, when we duplicated the experiment using equal-survival level dose of eptopside, another cancer chemotherapeutic drug that damages DNA, to treat the same cells, we did not observe such global transcription inhibition (Jun Yu and Haiying Hang, unpublished results). Therefore, DNA damage cannot be the sole reason why the global reduction of transcription was found only in HU-treated cells and other mechanisms may exist, such as changes of cell cycle and epigenetic regulation under HU treatment; we have failed to find any other relevant reports in the literature. Second, the elevated expression of ncRNAs, such as well-classified snoRNAs, snRNAs and srpRNAs, in response to HU treatment is of importance. A previous study suggested that snoRNAs are accumulated in cells under stress conditions (18); however, there has not been any report about the elevated transcriptional activity of snRNAs and srpRNAs in response to stress. Third, the change of alternative splicing in response to HU treatment supports the idea that transcription is coupled with alternative splicing (21). These transcriptomic changes are believed to be the hallmarks of the cellular response to HU treatment.

In our functional analyses, we proposed that HU treatment can arrest cell cycle at G_1/S phase possibly through the TGF-signaling pathway and transcriptional activation of *p15*, *p16* and *p21*. We further suggested that a possible mechanism for HU-mediated cell death could be induced by the tumor necrosis factor pathway and that the exonucleases *trex1*, *mus81*, *nthl1* and *xrcc1* play critical roles in HU-induced DNA damages. We made a novel discovery that cell communication and certain important signaling pathways are also influenced by HU treatment.

Evidently, the high-throughput sequencing technology can be used as a powerful tool to study mechanisms of therapeutic drugs at the transcriptome level. It provides adequate information on differential expressions of low-copy genes, such as via deeper sampling and can be used for studying transcriptome dynamics, including protein-coding and non-coding sequences. We suggested that the transcriptional alternation of non-coding sequences also offer additional information for novel mechanisms.

Supplementary material

Supplementary Figures S1–S13, Tables S1 and S2 and Files 1 and 2 can be found at http://carcin.oxfordjournals.org/

Funding

National Basic Research Program (973 Program) (2006CB910401, 2006CB910403 and 2006CB910404 to J.Y. and S.H.); National Protein Project of Ministry of Science and Technology (2006CB910902 to H.H.); Ministry of Science and Technology of the People's Republic of China; Knowledge Innovation Program of Chinese Academy of Sciences (KSCX2-YW-R63 and KJCX2-YW-L08 to H.H.); National Natural Science Foundation of China (30530180 to H.H.).

Acknowledgements

The authors especially would like to thank the Life Technologies' expert team Drs Xin Li, Hongying Yin, Jiandong Sun, Yangzhou Wang and Robert Nutter for their excellent technical supports.

Accession number: RNA-seq data has been submitted to NCBI SRA: SRA010068.

Conflict of Interest Statement: None declared.

References

1. Lanzkron,S. *et al*. (2008) Systematic review: hydroxyurea for the treatment of adults with sickle cell disease. *Ann. Intern. Med.*, **148**, 939–955.
2. Meo,A. *et al*. (2008) Effect of hydroxyurea on extramedullary haematopoiesis in thalassaemia intermedia: case reports and literature review. *Int. J. Lab. Hematol.*, **30**, 425–431.
3. Kennedy,B.J. (1992) The evolution of hydroxyurea therapy in chronic myelogenous leukemia. *Semin. Oncol.*, **19**, 21–26.
4. King,S. (2003) A role for nitric oxide in hydroxyurea-mediated fetal hemoglobin induction. *J. Clin. Invest.*, **111**, 171–172.
5. Koc,A. *et al*. (2004) Hydroxyurea arrests DNA replication by a mechanism that preserves basal dNTP pools. *J. Biol. Chem.*, **279**, 223–230.
6. Sakano,K. *et al*. (2001) Hydroxyurea induces site-specific DNA damage via formation of hydrogen peroxide and nitric oxide. *Jpn. J. Cancer Res.*, **92**, 1166–1174.
7. Hanft,V.N. *et al*. (2000) Acquired DNA mutations associated with *in vivo* hydroxyurea exposure. *Blood*, **95**, 3589–3593.
8. Cloonan,N. *et al*. (2008) Stem cell transcriptome profiling via massive-scale mRNA sequencing. *Nat. Methods*, **5**, 613–619.
9. Hopkins,K.M. *et al*. (2004) Deletion of mouse rad9 causes abnormal cellular responses to DNA damage, genomic instability, and embryonic lethality. *Mol. Cell. Biol.*, **24**, 7235–7248.
10. Hang,H. *et al*. (2004) Analysis of the mammalian cell cycle by flow cytometry. *Methods Mol. Biol.*, **241**, 23–35.
11. Singh,N. *et al*. (1988) A simple technique for quantitation of low levels of DNA damage in individual cells. *Exp. Cell Res.*, **175**, 184–191.
12. Olive,P. (1989) Cell proliferation as a requirement for development of the contact effect in Chinese hamster V79 spheroids. *Radiat. Res.*, **117**, 79–92.
13. Hu,Z. *et al*. (2008) Targeted deletion of Rad9 in mouse skin keratinocytes enhances genotoxin-induced tumor development. *Cancer Res.*, **68**, 5552.
14. Mortazavi,A. *et al*. (2008) Mapping and quantifying mammalian transcriptomes by RNA-Seq. *Nat. Methods*, **5**, 621–8.
15. Salomonis,N. *et al*. (2007) GenMAPP 2.: new features and resources for pathway analysis. *BMC Bioinformatics*, **8**.
16. Li,C. *et al*. (2001) Model-based analysis of oligonucleotide arrays: expression index computation and outlier detection. *Proc. Natl Acad. Sci. USA*, **98**, 31–36.
17. Zhang,C. *et al*. (2008) Phosphorylation sites on Tyr28 and the C-terminus of Rad9 are required for inhibition of premature chromosomal condensation across the entire s phase. *Cell. Physiol. Biochem.*, **22**, 295–306.
18. Chen,M.S. *et al*. (2002) Differential accumulation of U14 snoRNA and hsc70 mRNA in Chinese hamster cells after exposure to various stress conditions. *Cell Stress Chaperones*, **7**, 65–72.
19. Faulkner,G.J. *et al*. (2009) The regulated retrotransposon transcriptome of mammalian cells. *Nat. Genet.*, **41**, 563–571.
20. Guthrie,C. *et al*. (1988) Spliceosomal snRNAs. *Annu. Rev. Genet.*, **22**, 387–419.
21. Munoz,M.J. *et al*. (2009) DNA damage regulates alternative splicing through inhibition of RNA polymerase II elongation. *Cell*, **137**, 708–720.
22. Woo,G.H. *et al*. (2006) Molecular mechanisms of hydroxyurea(HU)-induced apoptosis in the mouse fetal brain. *Neurotoxicol. Teratol.*, **28**, 125–134.
23. Fallon,R.J. *et al*. (1979) Cell cycle analysis of sodium-butyrate and hydroxyurea, inducers of ectopic hormone production in HeLa cells. *J. Cell. Physiol.*, **100**, 251–261.
24. Xiong,Y. *et al*. (1993) P21 is a universal inhibitor of cyclin kinases. *Nature*, **366**, 701–704.
25. Musgrove,E.A. *et al*. (1995) Expression of the cyclin-dependent kinase inhibitors P16(Ink4), P15(Ink4b) and P21(Waf1/Cip1) in human breast-cancer. *Int. J. Cancer*, **63**, 584–591.
26. Lois,A.F. *et al*. (1995) Expression of the P16 and P15 cyclin-dependent kinase inhibitors in lymphocyte-activation and neuronal differentiation. *Cancer Res.*, **55**, 4010–4013.
27. Hannon,G.J. *et al*. (1994) P15(Ink4b) is a potential effector of Tgf-beta-induced cell-cycle arrest. *Nature*, **371**, 257–261.
28. Daniel,C. *et al*. (2004) Thrombospondin-1 is a major activator of TGF-beta in fibrotic renal disease in the rat *in vivo*. *Kidney Int.*, **65**, 459–468.
29. Derynck,R. *et al*. (2003) Smad-dependent and Smad-independent pathways in TGF-beta family signalling. *Nature*, **425**, 577–584.
30. Liu,J.H. *et al*. (1999) Functional association of TGF-beta receptor II with cyclin B. *Oncogene*, **18**, 269–275.
31. Sherr,C.J. *et al*. (1999) CDK inhibitors: positive and negative regulators of G(1)-phase progression. *Genes Dev.*, **13**, 1501–1512.
32. Katsuno,Y. *et al*. (2009) Cyclin A-Cdk1 regulates the origin firing program in mammalian cells. *Proc. Natl Acad. Sci. USA*, **106**, 3184–3189.
33. Hsu,H.L. *et al*. (1996) TRADD-TRAF2 and TRADD-FADD interactions define two distinct TNF receptor 1 signal transduction pathways. *Cell*, **84**, 299–308.
34. Bender,L. *et al*. (2005) The adaptor protein TRADD activates distinct mechanisms of apoptosis from the nucleus and the cytoplasm. *Cell Death Differ.*, **12**, 473–481.
35. Cho,S. *et al*. (2002) Apoptotic signaling pathways: caspases and stress-activated protein kinases. *J. Biochem. Mol. Biol.*, **35**, 24–27.
36. Mohan,S. *et al*. (2003) Ikappa B alpha-dependent regulation of low-shear flow-induced NF-kappa B activity: role of nitric oxide. *Am. J. Physiol. Cell Physiol.*, **284**, C1039–C1047.
37. Smirnov,D.A. *et al*. (2009) Genetic analysis of radiation-induced changes in human gene expression. *Nature*, **459**, 587–U120.
38. Han,J.W. *et al*. (2001) Expression of bbc3, a pro-apoptotic BH3-only gene, is regulated by diverse cell death and survival signals. *Proc. Natl Acad. Sci. USA*, **98**, 11318–11323.
39. Rodriguez,J.M. *et al*. (2006) Bok, Bcl-2-related ovarian killer, is cell cycle-regulated and sensitizes to stress-induced apoptosis. *J. Biol. Chem.*, **281**, 22729–22735.
40. Osman,F. *et al*. (2007) Exploring the roles of Mus81-Eme1/Mms4 at perturbed replication forks. *DNA Repair (Amst.)*, **6**, 1004–1017.
41. Sarker,A.H. *et al*. (1998) Cloning and characterization of a mouse homologue (mNthl1) of Escherichia coli endonuclease III. *J. Mol. Biol.*, **282**, 761–774.
42. Yang,Y.G. *et al*. (2007) Trex1 exonuclease degrades ssDNA to prevent chronic checkpoint activation and autoimmune disease. *Cell*, **131**, 873–886.
43. Kubota,Y. *et al*. (1996) Reconstitution of DNA base excision-repair with purified human proteins: interaction between DNA polymerase beta and the XRCC1 protein. *EMBO J.*, **15**, 6662–6670.
44. Whitehouse,C.J. *et al*. (2001) XRCC1 stimulates human polynucleotide kinase activity at damaged DNA termini and accelerates DNA single-strand break repair. *Cell*, **104**, 107–117.
45. Burley,S.K. *et al*. (1996) Biochemistry and structural biology of transcription factor IID (TFIID). *Annu. Rev. Biochem.*, **65**, 769–799.
46. Orphanides,G. *et al*. (1996) The general transcription factors of RNA polymerase II. *Genes Dev.*, **10**, 2657–2683.
47. Roeder,R.G. (1996) The role of general initiation factors in transcription by RNA polymerase II. *Trends Biochem. Sci.*, **21**, 327–335.
48. Berk,A.J. (1999) Activation of RNA polymerase II transcription. *Curr. Opin. Cell Biol.*, **11**, 330–335.
49. Danen,E.H.J. *et al*. (2001) Fibronectin, integrins, and growth control. *J. Cell. Physiol.*, **189**, 1–13.
50. Powers,C.J. *et al*. (2000) Fibroblast growth factors, their receptors and signaling. *Endocr. Relat. Cancer*, **7**, 165–197.
51. Hooper,J.E. *et al*. (2005) Communicating with Hedgehogs. *Nat. Rev. Mol. Cell Biol.*, **6**, 306–317.
52. Birchmeier,W. (2007) The Wnt/beta-catenin signaling pathway in development and disease. *Pathol. Res. Pract.*, **203**, 341–341.
53. Lee,K.B. *et al*. (2002) Transcription-coupled and DNA damage dependent ubiquitination of RNA polymerase II *in vitro*. *Proc. Natl Acad. Sci. USA*, **99**, 4239–4244.

Received January 13, 2010; revised April 27, 2010; accepted May 25, 2010